# Design, development, and manufacture of an aluminium honeycomb sandwich panel monocoque chassis for Formula Student competition

H C Davies, M Bryant, M Hope and C Meiller

*Proceedings of the Institution of Mechanical Engineers, Part D: Journal of Automobile Engineering* 2012 226: 325
originally published online 23 September 2011
DOI: 10.1177/0954407011418578

# Design, development, and manufacture of an aluminium honeycomb sandwich panel monocoque chassis for Formula Student competition

**H C Davies**[1]*, **M Bryant**[1], **M Hope**[1], and **C Meiller**[2]

[1]School of Engineering, Cardiff University, Cardiff, UK

[2]Institut Français de Mécanique Avancée, Clermont-Ferrand Les Cézeaux, Aubière, France

*The manuscript was received on 6 May 2011 and was accepted after revision for publication on 11 July 2011.*

DOI: 10.1177/0954407011418578

**Abstract:** Cardiff University students have used the freedom of the Formula Student rules to create an innovative chassis that combines a high performance with an efficient manufacturing process. All aluminium sandwich panels were pre-cut using computer numerical control routing, which is a rapid low-cost operation that produced highly accurate results. Assembling the monocoque consisted of folding and bonding panels along pre-routed lines and reinforcing the relevant joints. This required no specialist tools or equipment and was a rapid non-labour-intensive operation. The key design features, the manufacturing techniques, and the results of experimental and computational performance testing are presented here. This chassis construction technique is the result of research and development for seven years over six generations of Formula Student race cars.

**Keywords:** monocoque chassis, aluminium honeycomb, Formula Student, Formula SAE, race car safety

## 1 INTRODUCTION

Following the successful introduction of Formula SAE (FSAE) into the USA in 1979 [**1**], a similar European scheme called Formula Student (FS), managed by the Institution of Mechanical Engineers, was launched in 1998 [**2**]. The philosophy of both FSAE and FS is to enable students to demonstrate and prove their creativity and engineering skills through the design, manufacture, and financing of a small Formula-style race car.

In keeping with the above philosophy, chassis design requirements are prescriptive only in the sense that they seek to ensure a high level of competitor safety. This is achieved by defining a baseline space frame chassis and requiring that alternative chassis designs demonstrate equivalent energy dissipation, yield, and ultimate strengths in bending, buckling, and tension. This allows for innovative thinking in how to approach chassis design.

Cardiff Racing is the FS team of Cardiff University and is part of the Cardiff School of Engineering. Cardiff Racing has acquired a reputation for being consistently innovative in its approach to the design of its FS chassis, the cornerstone of this innovation being the move to an aluminium honeycomb chassis from the more ubiquitous space frame. Starting with CR01 (the first-generation race car) in 2004, Cardiff Racing has looked to increase the proportion of aluminium honeycomb used in chassis construction, while at the same time to ensure that the chassis construction method is both effective and economically viable. The present chassis construction technique is the result of research and development for seven years of over six generations of FS race cars. The extensive knowledge base developed at Cardiff University has been used to design a chassis that reduces manufacturing time (by reducing the fabrication requirements), improves performance (by

*Corresponding author: School of Engineering, Cardiff University, Room W/2.28, Queen's Buildings, Newport Road, Cardiff CF24 3AA, UK.
email: davieshc@cardiff.ac.uk

reducing the requirement for supplementary structures while enhancing performance), and reduces mass (by reducing material use).

The following sections describe experience in the design and manufacture of the aluminium honeycomb chassis and the results of experimental and numerical testing for the purpose of supporting design decisions and demonstrating equivalency to a baseline space frame chassis design.

## 2 DESIGN AND MANUFACTURE

### 2.1 Aluminium honeycomb sandwich panels

The use of sandwich panel construction techniques can be widely seen in modern-day Formula 1 chassis design but also extends into the marine and aerospace industries, which share similar requirements for their material choices [**3**]. The structural sandwich concept involves combining two thin and stiff faces with a thick and relatively weak core. The principle of sandwich construction is that the bending loads are carried by the skins, while the core transmits the shear load. They enable large gains in structural efficiency, since the thickness (and hence the flexural rigidity) of panels can be increased without significant weight penalty.

Potential materials for sandwich facings are aluminium alloys, high-tensile steels, titanium, and composites depending on the specific mission requirement. The most common face material in this category by far is sheet metal, which offers good properties at reasonable cost [**3**]. Several types of core shape and core material have been applied to the construction of sandwich structures. One type of core shape is honeycomb, which consists of very thin foils in the form of hexagonal cells perpendicular to the facings. The most common honeycomb cores are based on aluminium and aramid fibre paper dipped in phenolic resin, the latter having the trade name Nomex [**3**].

For the FS car described here, aluminium was the material choice for facings and core. The aluminium sandwich panel was Cellite 220 with aluminium grade 5251 H22/H24 face plates [**4**]. This was based on the requirements to account for costs in the design and manufacture (costs are assessed as part of the FS competition), and the requirement for a high strength-to-weight ratio (essential for a competition car). A further advantage is the ease of recycling the chassis at the end of life.

### 2.2 Design for manufacture

The chassis design for the sixth generation of FS car was deconstructed into component parts (Fig. 1).

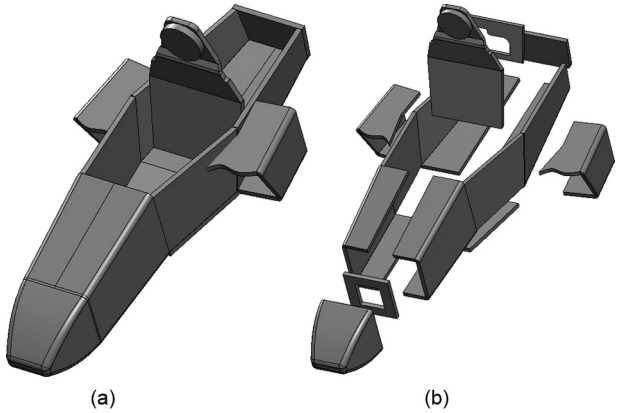


**Fig. 1** (a) CRO6 chassis showing the consolidated chassis; (b) the deconstructed chassis

The deconstruction was an iterative process. The number and shape of the component parts were based on minimizing the number of panels and the number of joints for both improved performance (resulting from a reduction in the vehicle mass) and more efficient manufacture (reductions in the time and the cost). Reducing the number of panels and/or joints in turn refined the design of the chassis.

The component parts were constructed from 'shaped' panels that have been cut from larger panels. The cutting of the shaped panels was performed with a computer numerical control (CNC) router–cutter using a file generated from a three-dimensional (3D) computer model of the chassis.

To facilitate folding, the shaped panels were routed along the fold lines. Routing consists of removing part of the facing panel and removing a section of the core material beneath. The width of the face plate removed defines the angle to which the panel can be folded. Therefore the panel is self-jigging (i.e. no supplementary jig is required to position the panel). The reason for removal of the core material is to prevent 'stacking' of the core material when the panel is folded.

Assembly of the component parts was by folding the shaped panels along the fold lines to the specified angle. To restore load path continuity a reinforcement plate was bonded to the inner facing plates with a two-part epoxy (Araldite 420 A/B [**5**]).

Assembly of the chassis was by joining the component parts. As for the folds, a two-part epoxy was used. However, a key difference was the requirement to bond reinforcement plates to both the outer and the inner skins to provide load path continuity.

The result is a chassis assembly process that is low cost, produces highly accurate results, and to a large extent is self-jigging, therefore removing the requirement for supplementary jigs to support the

assembly process. In addition, for the chassis design manufactured by Cardiff Racing the aluminium honeycomb monocoque was both the frame and the body of the race car, therefore removing the requirement for supplementary external panels.

### 2.3 Folds and joints

A comprehensive test programme has been undertaken to assess the strength of folds and joints to compressive and tensile loading. The panel used was a 30 mm composite panel (0.5 mm aluminium skin–29 mm aluminium honeycomb core–0.5 mm aluminium skin). The maximum angle for any fold or joint is 90°. To determine the strength of the 90° fold or joint, test specimens were subjected to quasi-static loading in either compression or tension. The test set-up for the tensile test is shown in Fig. 2. For the compressive test the direction of $F$ in Fig. 2 was reversed.

For the 90° fold, the average failure load was 920 N in compression and 720 N in tension. The load–deflection or load–extension curves can be seen in Appendix 2. In compression the failure was due to compression of the core material (Fig. 3(a)), while in tension it was due to debonding of the inner face plate (Fig. 3(b)). From the above, it is clear that the compressive strength of the core material was higher than that of the adhesive.

For the 90° joint, the average failure load was 465 N in compression and 395 N in tension (note that this load relates to the first observation of failure, and hence to the loss of function, and not to the peak load). The load–deflection or load–extension curves can be seen in Appendix 2. The lower

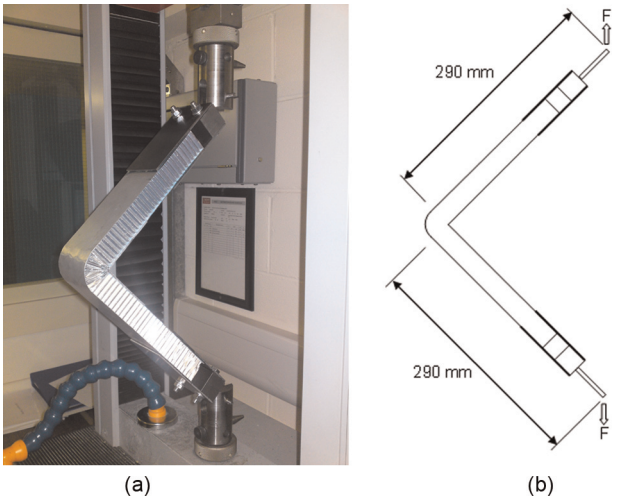


**Fig. 2** (a) Specimen inserted into the testing machine; (b) test dimensions (width, 75 mm; panel depth, 30 mm)

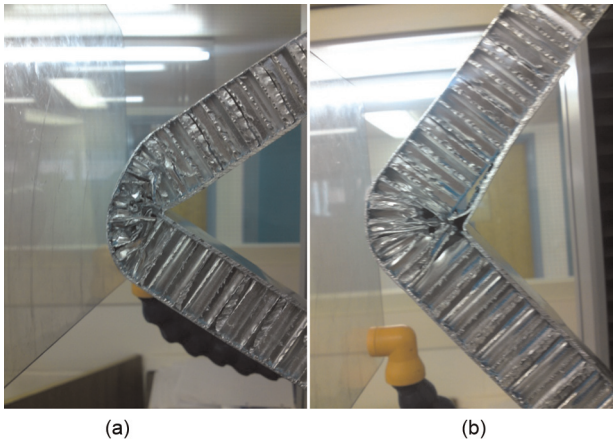


**Fig. 3** Failure modes of the 90° fold: (a) compressive loading; (b) tensile loading

failure load in these tests, in comparison with the 90° fold, was due to debonding of the outer-skin reinforcement plate from the exposed edge of the sandwich panel (Fig. 4). Once the skin had debonded, the stability of the core was compromised and the aluminium honeycomb would start to buckle.

Up to the point of failure, each arm of the fold or joint can be considered as a cantilevered beam, with the beam subject to a bending load and tensile load along the neutral axis. The normal stress in the face plate at the point of failure can be found by summing the stress due to the bending load according to

$$\mathrm{BM} = F\cos 45 \times l = \frac{\sigma I}{y} \tag{1}$$

and the stress due to the tensile load according to

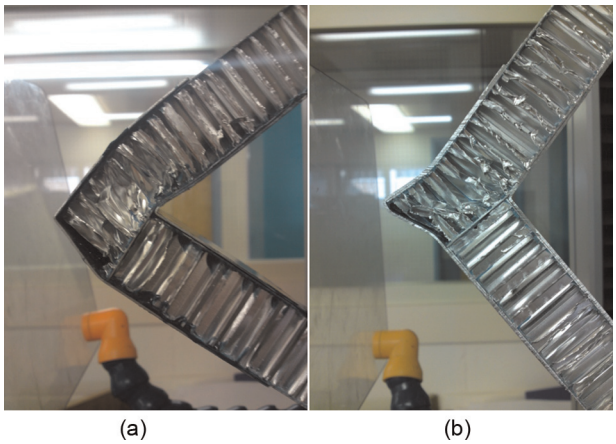


**Fig. 4** Failure modes of the 90° joint: (a) compressive loading; (b) tensile loading

**Table 1** Normal stresses in the face plate at the points of failure

| | | Normal stress (MPa) |
|---|---|---|
| 90° fold | Compression | 182.1 |
| | Tension | 142.5 |
| 90° joint | Compression | 92.0 |
| | Tension | 78.1 |

$$F \cos 45 = \sigma A \tag{2}$$

where BM is the bending moment (the applied load multiplied by the moment arm), $\sigma$ is the stress (due to the bending moment or the tension or compression force), $I$ is the second moment of area of the panel, $y$ is the distance from the neutral axis to the outer edge of the panel, $F$ is the applied force, and $A$ is the cross-sectional area (for an I-beam with a negligible web thickness this relates to the cross-sectional area of the two flanges). To simplify the problem, the sandwich panel was considered to represent an I-beam with a negligible web thickness.

The normal stress in the face plates for each of the test conditions is shown in Table 1.

The above values were taken to define the maximum allowable stress within a chassis joint or fold when subjected to tensile or compressive loading.

### 2.4 Inserts

Owing to the layered structure of sandwich plates, where two rigid, strong, and relatively dense face sheets are separated by a compliant and lightweight core material, structural sandwich panels are notoriously sensitive to the application of localized external loads [**6**]. Inserts are used for the transfer of localized external loads to the sandwich structure.

For the monocoque chassis present here, in-house designed and manufactured aluminium alloy 6082-T6 inserts will be used. The inserts are formed from two parts (one male and one female) and are bonded to the sandwich panel (Fig. 5). For the M8 insert (the centre hole would be 8 mm in diameter) the head is 30 mm in diameter and, when assembled, the outside diameter of the central part is 12 mm.

To provide design guidelines on the use of these inserts, a comprehensive test programme was undertaken to assess the strength of the inserts in shear loading and tensile or compressive loading when bonded to an aluminium honeycomb panel. A 25 kN Testometric M500 universal testing machine was used to load the insert in single-shear loading, double-shear loading, and tensile or compressive loading. The load rate was 5 mm/min. The test set-ups for the single-shear test and the pull-through test are shown in Fig. 6.

In single shear the failure load was 5.2 kN (averaged over three tests; see Appendix 3 for an example load–extension curve). The failure of the insert was due to debonding of the insert from the face plates of the sandwich panel, prior to the tearing of one of the face plates. In double shear, the strength of the connection was 9.1 kN (averaged over three tests). The higher strength of this connection was due to the necessity to initiate the tear in both the front and the rear face plate at the same time. The fact that the load was less than double that of the single-shear test may be explained in part by repeatability of the tests (the individual failure loads varying by ±1 kN about the average) and by the fact that, for

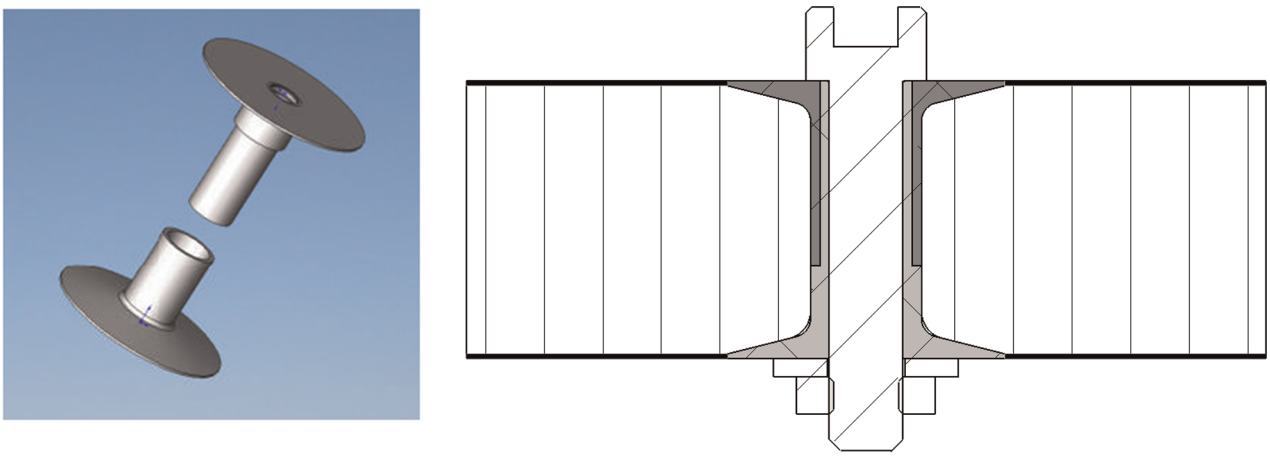


**Fig. 5** (a) The two-part insert; (b) the insert located in a sandwich panel

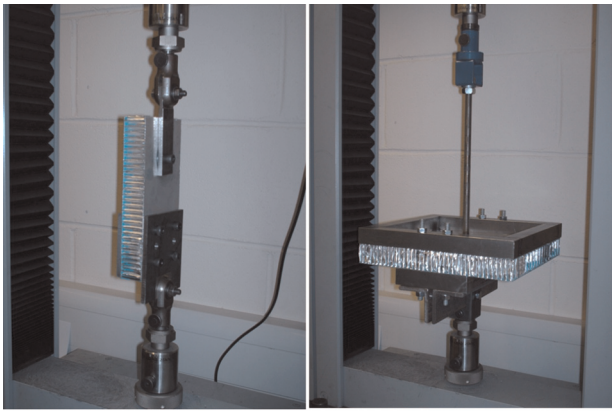


**Fig. 6** Insert test configuration

the single-shear test, debonding of the insert resulted in localized compression of the honeycomb core as the insert rotated because of the off-centre loading. A similar compression of the core material did not occur for the double-shear test.

For tensile or compressive loading, the failure load was 3.4 kN (averaged over three tests; see Appendix 3 for an example load–extension curve). The initial failure was due to debonding of the insert from the face plate on the side subject to tensile loading, prior to the insert shearing the face plate on the side subject to compressive loading. The use of a load-spreading plate (size, 60 mm × 40 mm) on the side subject to the compressive load was observed to increase the failure load to 9.8 kN (averaged over three tests) owing to the engagement of a larger area of the honeycomb core (Fig. 7).

## 3 PERFORMANCE EVALUATION

The performance evaluation of the monocoque was based on comparison with a baseline space frame chassis. The specification of the space frame chassis is defined by the FSAE and FS rules and ensures a minimum level of safety for the occupant in the event of a front impact, side impact, or rollover. Two equivalent space frame designs were modelled. These space frames have a similar geometry to that of a monocoque and are constructed of mild steel tubes. The only difference between the two designs is the direction of the diagonal members. Figure 8 shows the space frame chassis design.

The equivalent space frame models were constructed of two-node beam elements. The material was mild steel with an elastic modulus of 200 GPa, Poisson's ratio of 0.3, and a density of 7850 kg/m$^3$. The outside diameter and the wall thickness for the tubular sections were 25.4 mm and 2.4 mm respectively for the main roll hoop, front roll hoop, and shoulder harness mounting, 25.4 mm and 1.65 mm respectively for the front bulkhead, side impact structure, and roll hoop bracing, and 25.4 mm and 1.25 mm respectively for the front bulkhead support and transverse members.

In total, 14 individual load cases were analysed. For the main and front roll hoop load cases a 1 kN load was applied at top of main roll hoop in the vertical direction (downwards), in the horizontal direction along the car centre-line (forwards and backwards), and at 45° to the horizontal along the car centre-line (forwards and backwards). For the side impact loading, a 10 kN load was split into three and applied at the midpoint of each of the three side impact bars to simulate a side impact. For the front bulkhead loading, a 10 kN horizontal load was split into four and applied at each of the corners of the front bulkhead to simulate a frontal impact, a 1 kN vertical load was applied to each of the top two corners of the front bulkhead to simulate a vertical impact on the front of the car, and two opposing 1 kN horizontal forces were applied to opposite corners on the front bulkhead. A summary of the results is provided in Appendix 4.

### 3.1 Rollover

The primary safety device in the event of a rollover is the roll hoop. The FSAE and FS rules require a

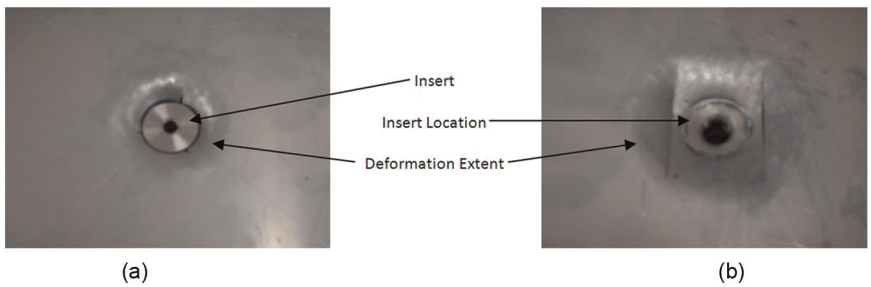


**Fig. 7** Insert pull-through test without the reinforcement plate ((a) insert in place) and with the reinforcement plate ((b) insert and plate removed for clarity). The deformation extent is greater with the addition of the reinforcement plate

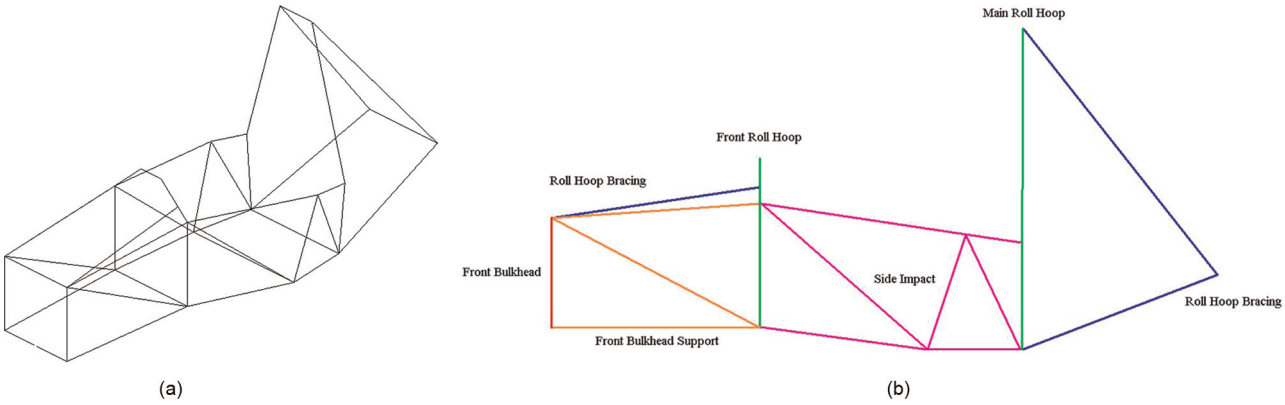


**Fig. 8** Equivalent space frame designs

front and a rear (main) roll hoop for both space frame and monocoque chassis designs. For a monocoque chassis, the strength of the attachment of the roll hoop to the chassis must equivalent to or greater than that of the space frame chassis roll hoop failure load.

The loading applied to the top of the roll hoop in a downward vertical direction was taken to represent a rollover crash event. The analysis of the finite element model of the space frame chassis predicted a failure load for the main roll hoop of 32 kN in buckling, while that of the front roll hoop was 134 kN in buckling.

For the monocoque chassis a vertical load applied downwards to the roll hoop would be shared by the connections attaching the roll hoop to the chassis side and the connections attaching the roll hoop to the chassis floor and the top surface of the chassis front structure (front hoop only). The side connections are via M8 12.9 bolts passing through bonded inserts. The limiting factor was determined as the insert shear strength (5.2 kN insert shear failure load compared with 36.8 kN bolt shear failure load). The floor and chassis front structure would be loaded in compression and a conservative estimate of the failure load would be the engagement area multiplied by the core crush strength (which was 4.6 MPa).

For the main roll hoop, there were eight connections to the chassis side, and the area subjected to compression was 10 272 $mm^2$. The connection strength was therefore 88.9 kN. For the front roll hoop there were eight connections and the area was 33 500 $mm^2$. The connection strength was therefore 196 kN. The connection strength was therefore greater than the predicted roll hoop failure load for both the main and the front roll hoops, demonstrating the suitability of the connection design.

For the front and rear roll hoops there is a requirement for there to be a triangulated structure to transmit the load from the bottom of the hoop bracing back to the roll hoop (see Fig. 8). For the monocoque design the load path is the aluminium honeycomb sandwich panel. To demonstrate the suitability of this connection the tensile, buckling, and bending strengths of the panel were calculated and compared with the values for the steel tube used for the baseline chassis.

For the baseline steel tube the tensile strength of this load path is given by

$$Y_{\mathrm{hb_{sf}}} = \frac{\pi\left(D^2_{\mathrm{hb_o}} - D^2_{\mathrm{hb_i}}\right)}{4}\sigma_{\mathrm{y_{ms}}} \tag{3}$$

the buckling strength (flexural stiffness) is given by

$$EI_{\mathrm{hb_{sf}}} = \frac{\pi\left(D^4_{\mathrm{hb_o}} - D^4_{\mathrm{hb_i}}\right)}{64}E_{\mathrm{ms}} \tag{4}$$

and the bending strength is given by

$$M_{\mathrm{hb_{sf}}} = \frac{\sigma_{\mathrm{y_{ms}}} I_{\mathrm{hb_{sf}}}}{0.5 D_{\mathrm{hb_o}}} \tag{5}$$

where $D_{\mathrm{hb_o}}$ and $D_{\mathrm{hb_i}}$ are the outside and inside diameters respectively of the tube forming the hoop-brace load path, $\sigma_{\mathrm{y_{ms}}}$ is the yield strength for mild steel, $E_{\mathrm{ms}}$ is the modulus of elasticity for mild steel, and $I_{\mathrm{hb_{sf}}}$ is the second moment of area. It should be noted that the subscript hb is used to denote the values related to the hoop-brace load path and the subscript sf is used to denote the space frame chassis.

For the mild steel tube, given a yield strength of 235 MPa, a modulus of elasticity of 200 GPa, an outer diameter of 25.4 mm, and an inner diameter of 22.1 mm, the load path tensile, buckling, and bending strengths are as shown in Table 2.

**Table 2** Tensile, buckling, and bending strengths for the aluminium sandwich panel and mild steel tube hoop-brace load paths

| | Values for the following | | |
|---|---|---|---|
| | Mild steel tube | Aluminium sandwich panel | |
| | | Front | Rear |
| Tensile strength | 28.9 kN | 43.7 kN | 87.4 kN |
| Buckling strength | 1744 N m$^2$ | 2894 N m$^2$ | 5788 N m$^2$ |
| Bending strength | 161 N m | 717 N m | 717 N m |

The sandwich panel can be considered as an aluminium I-beam with a negligible web thickness. The tensile strength of this load path is given by

$$Y_{\mathrm{hb_m}} = 2t_{\mathrm{s}} b_{\mathrm{hb}} \sigma_{\mathrm{y_{Al}}} \tag{6}$$

the buckling strength (flexural stiffness) is given by

$$EI_{\mathrm{hb_m}} = \frac{b_{\mathrm{hb}}\left[d_{\mathrm{p}}^3 - \left(d_{\mathrm{p}} - 2t_{\mathrm{s}}\right)^3\right]}{12} E_{\mathrm{Al}} \tag{7}$$

and the bending strength is given by

$$M_{\mathrm{hb_m}} = \frac{\sigma_{\mathrm{y_{Al}}} I_{\mathrm{hb_m}}}{0.5 d_{\mathrm{p}}} \tag{8}$$

where $t_{\mathrm{s}}$, $b_{\mathrm{hb}}$, and $d_{\mathrm{p}}$ are the panel skin thickness, the plate width, and the panel depth respectively (Fig. 9), $\sigma_{\mathrm{y_{Al}}}$ is the yield strength of aluminium, $E_{\mathrm{Al}}$ is the modulus of elasticity of aluminium, and $I_{\mathrm{hb_m}}$ is the second moment of area. The subscript hb is used to denote the values related to the hoop-brace load path and the subscript m is used to denote a monocoque chassis.

For the sandwich panel, given a yield strength of 220 MPa, a modulus of elasticity of 70 GPa, a flange thickness of 0.5 mm, and widths of 380 mm and 190 mm for the rear roll hoop load path and the front roll hoop load path respectively, the tensile, buckling, and bending strengths are as shown in Table 2.

The tensile, buckling, and bending strengths for the monocoque chassis are higher than for the space frame chassis, demonstrating the higher performance of the monocoque design.

It should be noted that, in comparing the performances of the space frame and monocoque, the yield stress is used as opposed to the ultimate tensile stress as the yield of a structure is taken to represent a loss or compromise in function. The *EI* value is used as the geometry and boundary conditions are shared between the space frame chassis and monocoque chassis.

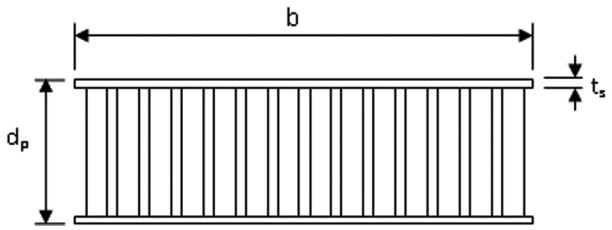


**Fig. 9** Aluminium honeycomb panel dimensions

### 3.2 Front structure

The primary safety device in the event of a frontal impact is the crash attenuator (an energy-absorbing device to limit the acceleration). In addition, there is a requirement to ensure that the structure behind the attenuator has sufficient strength to prevent intrusion into space set aside for the occupant. The strength of the monocoque front structure must be demonstrated to be equivalent to, or greater than, the baseline space frame chassis defined in the FSAE and FS rules. This includes the bulkhead and the supporting structure.

For the monocoque chassis an aluminium honeycomb panel was used for the front bulkhead rather than a bulkhead made from baseline steel tubing. The requirement was to demonstrate that the front bulkhead for the monocoque was equivalent to a space frame design.

Using the relationship

$$F = \frac{2\sigma I}{Ly} \tag{9}$$

where $F$ is the applied load, $\sigma$ is the stress, $I$ is the second moment of area, $L$ is the span, and $y$ is the distance from the neutral axis, the load required to cause yield through bending about each axis can be calculated.

For the space frame the bulkhead was formed from four mild steel tubes arranged to form a square frame with a span $L_x$ in the $x$ direction of 310 mm and a span $L_y$ in the $y$ direction of 325 mm. This is

**Table 3** Tensile, buckling, and bending strengths for the aluminium sandwich panel and mild steel tube bulkhead supports

| | Values for the following | |
|---|---|---|
| | Space frame chassis | Monocoque chassis |
| Tensile strength | 66.9 kN | 84.9 kN |
| Buckling strength | 4160 N m$^2$ | 5879 N m$^2$ |
| Bending strength | 385 N m | 1232 N m |

identified as the front bulkhead in Fig. 8. The tubes have a yield stress of 235 MPa, an outer diameter of 25.4 mm, and an inner diameter of 22 mm. The loads required to cause yield through bending were therefore 4.1 kN and 3.9 kN respectively.

In comparison, for the monocoque bulkhead the structure was formed from an aluminium honeycomb sandwich panel. The panel was 335 mm high by 350 mm wide with a section 190 mm high by 200 mm wide removed from the centre. This gives a span $L_x$ in the $x$ direction of 262.5 mm and a span $L_y$ in the $y$ direction of 275 mm. The faceplates of the sandwich panel have a yield stress of 220 MPa, a thickness of 0.5 mm, and a separation of 29 mm. For the second moment of area the sandwich panel was considered as an I-beam with a negligible web thickness. The loads required to cause yield through bending were therefore 4.3 kN and 3.9 kN respectively. The aluminium honeycomb panel bulkhead therefore had an equivalent performance to that of the baseline space frame chassis.

There are two supports for the bulkhead in the space frame design, one on each side of the vehicle consisting of three mild steel tubes with a yield strength of 235 MPa, a modulus of elasticity of 200 GPa, an outer diameter of 25.4 mm, and an inner diameter of 22.9 mm. This is identified as the front bulkhead support in Fig. 8. Using equations (3) to (5), the tensile, buckling, and bending strengths for the bulkhead supports can be found. These are shown in Table 3.

For the monocoque the equivalent support structure was the front side panel. The sandwich panel can be considered as an aluminium I-beam with a yield strength of 220 MPa, a modulus of elasticity of 70 GPa, a flange thickness of 0.5 mm, a minimum flange width of 386 mm, and a negligible web thickness. Using equations (6) to (8), the tensile, buckling, and bending strengths for the bulkhead supports can be found. These are shown in Table 3.

The tensile, buckling, and bending strengths for the monocoque chassis are higher than those for the space frame chassis, demonstrating the higher performance of the monocoque design. The floor and top panels would also contribute to the tensile, buckling, and bending strengths. Therefore the values given for the monocoque chassis can be considered conservative.

### 3.3 Side structure

The side structure should prevent intrusion into the occupant compartment in the event of a side impact. Intrusion in this context includes both catastrophic failure of the side structure and also localized penetration. As for rollover and frontal impact, the performance of the monocoque chassis should be demonstrated to be equivalent to, or greater than, that of the baseline space frame chassis.

For prevention of localized intrusion, the perimeter shear strength of the monocoque laminate should be at least 7.5 kN for a section with a diameter of 25 mm. For the sandwich panel used for construction of the monocoque (0.5 mm face plates), the shear strength of the face plates is 130 MPa. Therefore the load required to shear the face plate would be 5.1 kN. To prevent intrusion, the inner skin of the panel was supplemented by the bonding of an additional aluminium plate to increase the overall width of the faceplate to 1 mm and hence to increase the failure load to 10.2 kN.

For the space frame chassis, the side impact structure consists of three mild steel tubes with a yield strength of 235 MPa, a modulus of elasticity of 200 GPa, an outer diameter of 25.4 mm, and an inner diameter of 22.1 mm. This is identified as the side impact structure in Fig. 8. Using equations (3) to (5) the tensile, buckling, and bending strengths for the bulkhead supports can be found. These are shown in Table 4.

For the monocoque the equivalent structure was an aluminium honeycomb sandwich panel. The sandwich panel can be considered as an aluminium I-beam with a yield strength of 220 MPa, a modulus of elasticity of 70 GPa, flange thicknesses of 0.5 mm and 1 mm, a minimum flange width of 386 mm, and a negligible web thickness. Using equations (6) to (8) the tensile, buckling, and bending strengths for

**Table 4** Tensile, buckling, and bending strengths for the aluminium sandwich panel and mild steel tube side impact structure

| | Values for the following | |
|---|---|---|
| | Space frame chassis | Monocoque chassis |
| Tensile strength | 86.8 kN | 127.4 kN |
| Buckling strength | 5230 N m$^2$ | 5879 N m$^2$ |
| Bending strength | 484 N m | 1232 N m |

the bulkhead supports can be found. These are shown in Table 4.

The tensile, buckling, and bending strengths for the monocoque chassis are higher than those for the space frame chassis, demonstrating the higher performance of the monocoque design. The floor panel would also contribute to the tensile, buckling, and bending strengths, as would the structures containing the cooling radiator and electronics (more commonly referred to as the sidepods). These structures are of the same material as the chassis and are bonded to the chassis, therefore contributing greatly to its strength. Therefore the values given for the monocoque chassis can be considered conservative.

### 3.4 Finite element analysis

Simple hand calculations are useful to indicate the way in which elements of the monocoque structure will behave. However, the geometry of the structure and the use of composite materials mean that such calculations would become extremely complicated in considering the strength of the entire car. Finite element analysis (FEA) has therefore been carried out using MSC Patran/Nastran software to gain further understanding of the way in which the monocoque design would perform for a variety of load cases.

The aim of the analysis was to obtain the yield and buckling loads for the monocoque design and to compare these with the yield loads for the baseline space frame chassis. To this end a simplified model of the monocoque design has been created, as shown in Fig. 10.

The details of the modelling of the front and main roll hoops and the main roll hoop bracing are the same as for the space frame chassis discussed previously. The monocoque was modelled using a combination of four-node quadrilateral elements and three-node triangular elements. The main monocoque structure including the front bulkhead, rear floor, and seat consisted of a 30 mm composite panel (0.5 mm aluminium skin–29 mm honeycomb core–0.5 mm aluminium skin). At the front and main roll hoop attachment points the composite panel included the roll hoop mounting brackets (2 mm steel plate–0.5 mm aluminium skin–29 mm honeycomb core–0.5 mm aluminium skin). The composite panel was built up by specifying the material properties and thicknesses of the various layers of which it consists. The aluminium skin had an elastic modulus of 70 GPa, Poisson's ratio of 0.33, a shear modulus of 26.9 GPa, and a density of 2690 kg/m$^3$. The honeycomb core was specified as a 3D orthotropic material with properties as given in Table 5. The elastic moduli in the *xx* and *yy* directions are negligible and so were taken as 1 Pa as a value of zero would lead to a numerical failure.

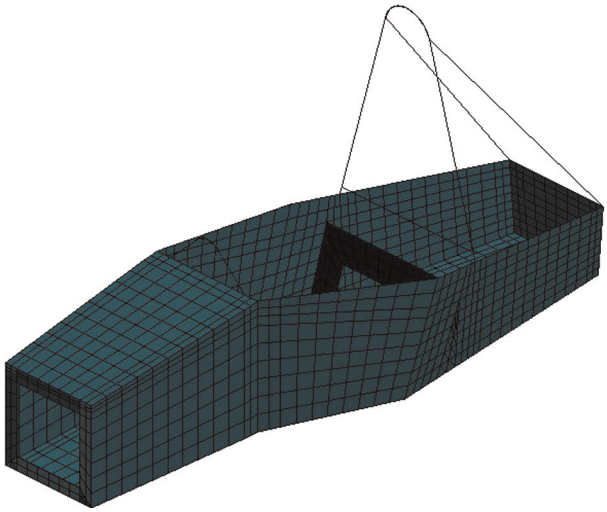

**Fig. 10** Finite element model of the aluminium honeycomb monocoque

In order to validate the FEA modelling approach and the chosen mesh density, a simple three-point bending test of a composite panel was performed. A section of aluminium honeycomb sandwich panel 30 mm thick was loaded with a 1 kN force at the midpoint of two supports. In the physical testing, a deflection of 0.57 mm was recorded. The test was recreated using the finite element software. The result of the FEA gave a deflection of 0.567 mm. The difference between the results of the physical testing and of the FEA was less than 1 per cent and validated the proposed approach (and the chosen mesh density).

In order to obtain the yield load for a given load case, a linear static analysis was carried out. The same load cases used for the models of the equivalent space frames as described previously were also applied to the model of the monocoque chassis. An image from the linear static analysis is shown in Fig. 11.

For the monocoque the maximum von Mises stress was obtained. The yield load for the monocoque could then be calculated as

$$\text{Yield load} = \frac{\text{allowable stress}}{\text{maximum von Mises stress}} \times \text{applied load} \tag{10}$$

Tests conducted at Cardiff University provided design guidelines for the maximum allowable stress (Table 1). For the monocoque design presented here, the maximum allowable stress was taken as

**Table 5** Aluminium honeycomb properties

| Property | Value |
|---|---|
| Elastic modulus 11 | 1 Pa |
| Elastic modulus 22 | 1 Pa |
| Elastic modulus 33 | 1000 MPa |
| Poisson's ratio 12 | 0.0003 |
| Poisson's ratio 23 | 0.0003 |
| Poisson's ratio 31 | 0.0003 |
| Shear modulus 12 | 1 MPa |
| Shear modulus 23 | 220 MPa |
| Shear modulus 31 | 220 MPa |
| Density | 80 kg/m$^3$ |

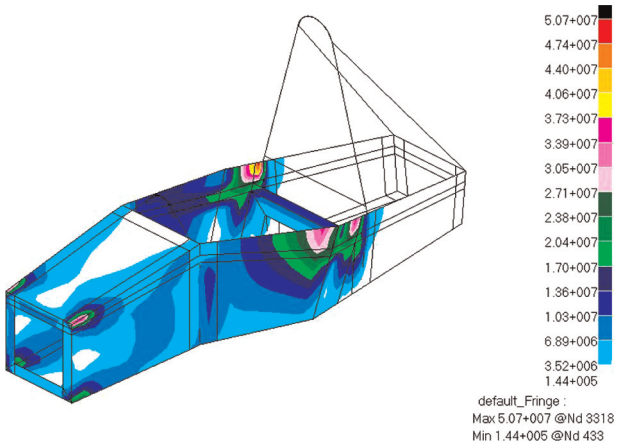


**Fig. 11** The von Mises stress distribution in an aluminium skin layer for horizontal loading of the front bulkhead (units in Pascals)

142.5 MPa, which is the normal stress in a 90° fold at the point failure. The basis for this decision was that all angles greater than 10° in the critical chassis areas are a result of folds and not joints (the stress in a 90° joint being less than that of a fold).

A similar approach was taken for the space frame using the tensile stress in place of the von Mises stress.

The lowest buckling load for each load case (monocoque and space frame) was obtained directly from a buckling analysis. The results of the analysis are shown in Tables 6 to 9.

In all but two load cases the monocoque chassis demonstrated superior performance (up to 3.4 times that of the dimensionally equivalent space frame). For the two load cases demonstrating inferior performances the stress distribution was investigated in more detail. For the forward load to the front structure, the maximum stress was observed to be on the outer skin in the area of cockpit aperture. For the downward load, the maximum stress was in the mild steel bulkhead (part of the main roll hoop). In both cases the stress in a fold was found to be less and resulted in a safety factor of greater than 1.

## 4 FURTHER CONSIDERATIONS

The FS and FSAE rules are continually evolving to provide enhanced competitor safety. The performance evaluation was based on a comparison of the sixth-generation Cardiff Racing car against the space frame chassis as defined in the 2010 FS rules and deals with the side, front, and rollover impact events. For entry into the competition, there are a number of additional equivalency rules that need to be considered. The chassis is compliant with these rules, but this has not been included as part of the above performance evaluation.

## 5 CONCLUSIONS

The chassis presented is a full monocoque, constructed from a 30 mm aluminium sandwich panel throughout. The assembly from flat sheet as described here has a number of advantages: no specialized tooling is required; existing technological CNC equipment may be used; the material quality is assured by the supplier, and not the manufacturer; direct integration between computer-aided design drawing, FEA, and computer-aided manufacturing is straightforward. Further to this, the construction technique removes the requirement for supplementary assembly jigs and, for the design presented here, the requirement for supplementary body panels. These advantages have obvious implications for capital and production costs.

The chassis design is the sixth generation produced by Cardiff Racing. The design has been supported by extensive hand calculations, finite element modelling, and physical testing to prove that it is structurally equivalent to a space frame. The results show that, in certain load cases, the predicted failure load for the monocoque chassis is up to 3.4 times greater than that of a dimensionally equivalent space frame chassis.

This chassis construction technique is the result of research and development for seven years over six generations of FS race cars. In developing the monocoque chassis, there is scope to enhance the performance while reducing the chassis weight and the cost and improving the efficiency of the manufacturing process. Areas that will be studied by future Cardiff Racing design teams include the following: material performance with changes to the face plates and panel width; joint design with changes to the reinforcement plate material and size; complex loading; the long-term performance of the chassis, particularly with regard to the adhesive fatigue and the effect of vibrations.

**Table 6** Loads applied to the main roll hoop

| Load applied | Yield load (kN) | | Buckling load (kN) | | Safety factor (lowest) |
|---|---|---|---|---|---|
| | Monocoque | Space frame | Monocoque | Space frame | |
| Downwards | 16.0 | 4.7 | 136.2 | 32.2 | 3.4 |
| Forwards | 6.8 | 1.1 | 49.0 | 41.0 | 1.2 |
| 45° forwards | 10.3 | 1.5 | 70.7 | 37.7 | 1.9 |
| Backwards | 6.8 | 1.1 | 49.0 | 41.0 | 1.2 |
| 45° backwards | 8.4 | 1.5 | 66.5 | 34.5 | 1.9 |

**Table 7** Loads applied to the front roll hoop

| Load applied | Yield load (kN) | | Buckling load (kN) | | Safety factor(lowest) |
|---|---|---|---|---|---|
| | Monocoque | Space frame | Monocoque | Space frame | |
| Downwards | 14.8 | 3.9 | 216.6 | 134.0 | 1.6 |
| Forwards | 5.9 | 4.3 | 344.3 | 98.5 | 1.4 |
| 45° forwards | 7.6 | 5.9 | 300.2 | 119.9 | 1.3 |
| Backwards | 5.9 | 4.3 | 344.3 | 98.5 | 1.4 |
| 45° backwards | 7.5 | 5.3 | 293.4 | 116.1 | 1.4 |

**Table 8** Loads applied to the side structure

| Load applied | Yield load (kN) | | Buckling load (kN) | | Safety factor (lowest) |
|---|---|---|---|---|---|
| | Monocoque | Space frame | Monocoque | Space frame | |
| Horizontal | 10.6 | 3.9 | 798.3 | 169.8 | 2.7 |

**Table 9** Loads applied to the front structure

| Load applied | Yield load (kN) | | Buckling load (kN) | | Safety factor (lowest) |
|---|---|---|---|---|---|
| | Monocoque | Space frame | Monocoque | Space frame | |
| Forwards | 27.7 | 48.2 | 632.3 | 100.5 | 0.6 |
| Downwards | 4.6 | 5.2 | 136.2 | 42.3 | 0.9 |
| Torsion | 18.5 | 5.4 | 805.2 | 114.0 | 3.4 |

## FUNDING

This research received no specific grant from any funding agency in the public, commercial, or not-for-profit sectors.

## ACKNOWLEDGEMENTS

The above work was undertaken in collaboration with the students of Cardiff University involved with the Automotive Design module. The design team for the sixth-generation monocoque chassis was J. Huber, K. Hodgson, J. Hursthouse, M. Pemberton, T. Roblin, L. Stevens, D. Walters, and L. Whitelegg.



## REFERENCES

1 Formula SAE, SAE Collegiate Design Series, About Formula SAE, 2010, available from http://students.sae.org/competitions/formulaseries/about.htm (accessed October 2010).

2 Institution of Mechanical Engineers, Formula Student, What is Formula Student?, 2010, available from http://www.formulastudent.com/aboutus/history (accessed 4 August 2011).

3 **Karlsson, K. F.** and **Åström, B. T.** Manufacturing and applications of structural sandwich components. *Composites Part A: Appl. Sci. Mfg*, 1997, **28**(2), 97–111.

4 AmberComposites, Cellite 220 metal & 620 fiber panels, Honeycomb sandwich panels, Issue ref: PDS/Cellite220metal&620fiberpanels/01, 9 August 2009.

5 AmberComposites, ARALDITE 420 A/B, 2 component epoxy adhesive, Issue Ref: TDS/ARALDITE420/01, 9 September 2009.

6 **Thomsen, O. T.** Load introduction aspects and localised bending phenomena in lightweight sandwich structures. In Proceedings of a Workshop on *The modelling of sandwich structures and adhesive bonded joints*, DOGMA (Design Guidelines and

Optimisation for Multimaterial Applications), Thematic Network under the European Commission, Porto, Portugal, 17–18 September 1998, pp. 1–5 (Aalborg Universitetsforlag, Aalborg).

## APPENDIX 1

### Notation

| | |
|---|---|
| $A$ | cross-sectional area |
| $b$ | sandwich panel width |
| BM | bending moment |
| $d$ | sandwich panel depth |
| $D_i$ | space frame tube diameter (inner) |
| $D_o$ | space frame tube diameter (outer) |
| $E$ | Young's modulus |
| $EI$ | flexural stiffness |
| $F$ | force |
| $I$ | second moment of area |
| $L$ | span |
| $M$ | bending strength |
| $t$ | sandwich panel skin thickness |
| $y$ | distance to neutral axis |
| $Y$ | yield strength |
| $\sigma$ | normal stress |

*Subscripts*

| | |
|---|---|
| Al | aluminium |
| hb | hoop brace |
| m | monocoque |
| ms | mild steel |
| sf | space frame |

## APPENDIX 2

### Joint tests and fold tests

Figures 12, 13, 14, and 15 show the example load–deflection or load–extension curves for compression tests on a 90° fold, for tensile tests on a 90° fold, for a compressive test on a 90° joint, and for tensile tests on a 90° joint respectively.

## APPENDIX 3

### Insert tests

Figures 16 and 17 show the example load–extension curves for an insert in single shear and for an insert pull-through test respectively.

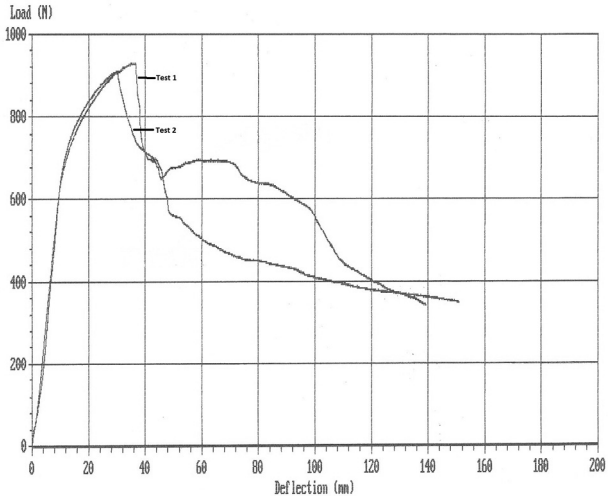


**Fig. 12** Example load–deflection curves for compression tests on a 90° fold

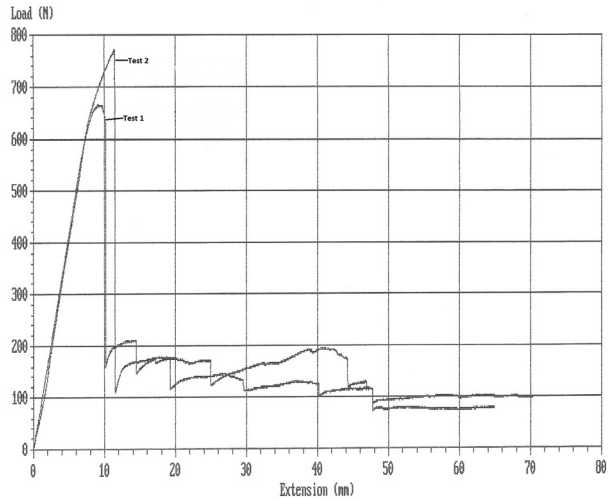


**Fig. 13** Example load–extension curves for tensile tests on a 90° fold

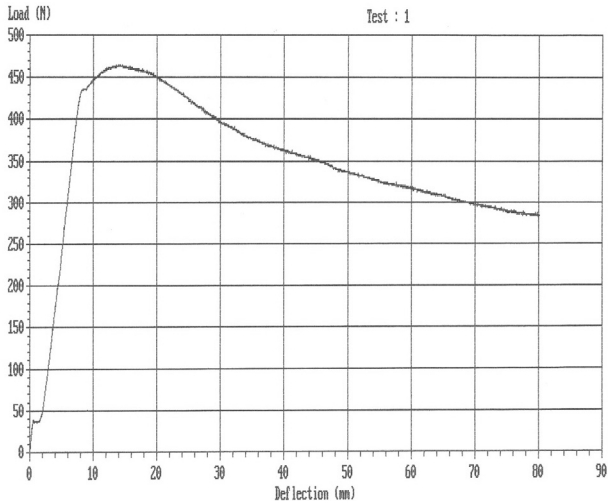


**Fig. 14** Example load–deflection curve for a compressive test on a 90° joint

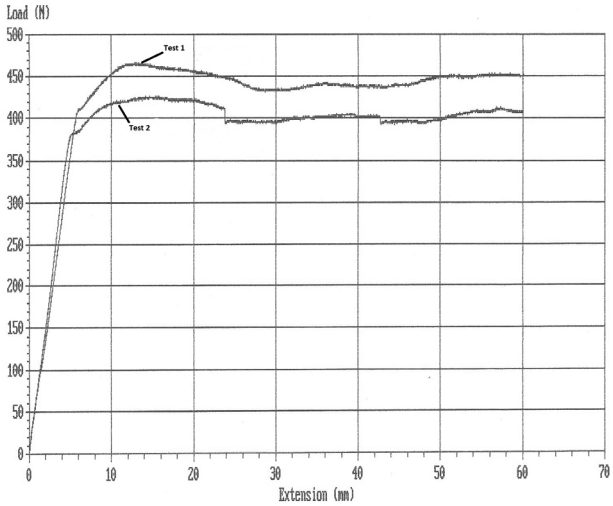


**Fig. 15** Example load–extension curves for a tensile test on a 90° joint

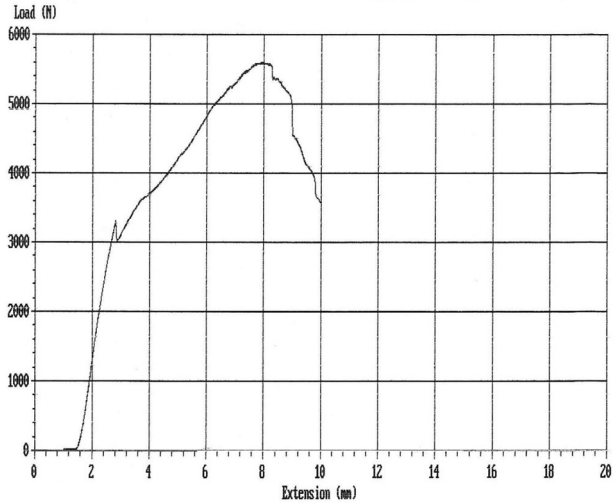


**Fig. 17** Example load–extension curve for an insert pull-through test

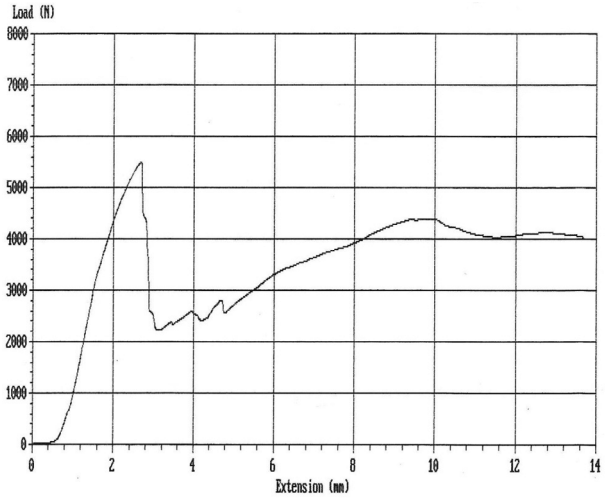


**Fig. 16** Example load–extension curve for an insert in single shear

## APPENDIX 4

## Space frame FEA

Table 10 gives a summary of the results for equivalent space frame chassis designs.

**Table 10** Summary of the results for equivalent space frame chassis designs

| Member loaded | Load applied | Design 1 | | | Design 2 | | |
|---|---|---|---|---|---|---|---|
| | | Buckling load (kN) | Maximum tensile stress (MPa) | Yield load (kN) | Buckling load (kN) | Maximum tensile stress (MPa) | Yield load (kN) |
| Main roll hoop | 1 kN vertically | 139.15 | 41.2 | 5.70 | 32.18 | 49.8 | 4.72 |
| | 1 kN horizontally forwards | 39.42 | 220 | 1.07 | 40.97 | 214 | 1.10 |
| | 1 kN at an angle of 45° forwards | 56.95 | 154 | 1.53 | 37.72 | 151 | 1.56 |
| | 1 kN horizontally backwards | 39.42 | 223 | 1.05 | 40.97 | 217 | 1.08 |
| | 1 kN at an angle of 45° backwards | 53.83 | 155 | 1.52 | 38.40 | 150 | 1.57 |
| Front roll hoop | 1 kN vertically | 216.62 | 59.8 | 3.93 | 134.01 | 58.8 | 4.00 |
| | 1 kN horizontally forwards | 344.25 | 54.7 | 4.30 | 101.33 | 54.6 | 4.30 |
| | 1 kN at an angle of 45° forwards | 300.20 | 39.9 | 5.89 | 119.85 | 39.1 | 6.01 |
| | 1 kN horizontally backwards | 344.25 | 54.8 | 4.29 | 101.33 | 54.8 | 4.29 |
| | 1 kN at an angle of 45° backwards | 293.42 | 44.7 | 5.26 | 116.09 | 44.1 | 5.33 |
| Side impact | 10 kN horizontally | 79.25 | 604 | 0.39 | 16.98 | 603 | 0.39 |
| Front bulkhead | 10 kN horizontally, shared four corners | 61.51 | 41.9 | 5.61 | 10.05 | 48.8 | 4.82 |
| | 1 kN vertically at top two corners | 67.34 | 63.6 | 3.69 | 21.14 | 90.5 | 2.60 |
| | 1 kN horizontally at opposite corners | 392.92 | 62.8 | 3.74 | 57.02 | 86.7 | 2.71 |